Journal of Visualization, Vol. 6, No. 3 (2003) 253-262

Planar Velocity Visualization in High-Speed Wedge Flow using Doppler Picture Velocimetry (DPV) compared with Particle Image Velocimetry (PIV)

Seiler, F.*, Havermann, M.*, George, A.*, Leopold, F.* and Srulijes, J.*

* French-German Research Institute of Saint-Louis (ISL)
5, Rue du Général Cassagnou, F-68301 Saint-Louis, France.
Tel: +33-3-8969-5042 / Fax: +33-3-8969-5048 / E-mail: seiler@isl.tm.fr

Received 6 November 2002
Revised 22 January 2003

Abstract : A technique for visualizing a velocity field in an entire plane has been developed by taking "Doppler Pictures" using Michelson interferometry. With the Doppler Picture Velocimetry (DPV), information about the instantaneous and local velocities of tracers passing through a light sheet is available. The technique for taking and processing the Doppler pictures has been improved recently and the state-of-the-art of the DPV method will be described with an application in high-speed fluid flows showing the velocity distribution in a light sheet plane crossing a supersonic wedge flow generated in the high-energy shock tunnel STB of ISL. A comparison with Particle Image Velocimetry (PIV) velocity visualizations is also presented.

Keywords : Light sheet, Tracer, Wedge flow, DPV picture, PIV image.

1. Introduction

Some measurement techniques have been developed for measuring a velocity distribution in a light sheet plane that illuminates a gas flow. A well-known technique is Particle Image Velocimetry (PIV) which is an often used tool for this purpose (Merzkirch, 1990). Another technique is Doppler Global Velocimetry (DGV), which uses an amplitude light filter for analyzing the Doppler shift of the frequency of the light scattered by tracer particles (Meyers, 1992). At the ISL, a special Michelson interferometer was designed (Oertel et al., 1982) to transform the Doppler shift of the frequency of the light scattered by tracer particles passing a light sheet into a shift of the light intensity leaving the interferometer. The changes in the light intensity distribution can be directly related to the velocities of the tracer particles. This method, called Doppler Picture Velocimetry (DPV), was further developed during recent years (Seiler et al., 1987; 1991, 1998) and the actual status of the DPV set-up and the technique for processing the interference image of the Doppler picture will be described herein. Some details on the progress in image processing have already been described by Seiler et al. (1999) and Leopold et al. (2000).

2. Principles of the DPV Technique

2.1 Doppler Effect

In order to measure the tracer velocity $\vec{v}$ in gases by the Doppler effect, the well-known relation of single-beam velocimetry is used as given in Equation (1) with the unit vectors $\vec{e}_L$ and $\vec{e}_D$. In Fig. 1, the vector $\vec{e}_L$ denotes the direction of illumination by the light source (L), and the vector $\vec{e}_D$ is directed from the tracers to the Michelson interferometer detector (D). θ is the angle between the two unit vectors $\vec{e}_L$ and $\vec{e}_D$. The velocity component of the flow vector $\vec{v}$ is measured in the direction of the difference vector $\vec{e}_D - \vec{e}_L$ which forms the angle γ to the velocity vector $\vec{v}$, as shown in Fig. 1. The Doppler frequency shift can be deduced with the Doppler effect relations as follows:

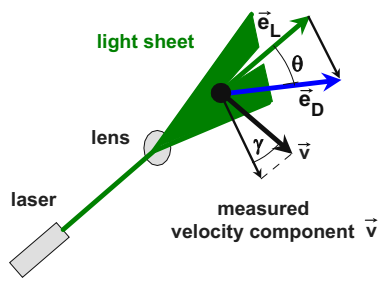

Fig. 1. Doppler effect.

$$\frac{dv_L}{v_L} = \frac{\vec{v}\left(\vec{e}_D - \vec{e}_L\right)}{c} = 2\frac{v}{c}\cos\gamma \sin\frac{\theta}{2} \tag{1}$$

The laser light source frequency is denoted by ν_L. By the Doppler effect that frequency is shifted to ν_D and the frequency shift $d\nu_L = \nu_D - \nu_L$ is analyzed via the Michelson interferometer.

2.2 Operation of the Michelson Interferometer

A plane crossing the gas flow is illuminated by a light sheet with frequency ν_L. In order to visualise the velocity distribution in this plane, tracer particles are seeded into the flow and the light scattered from these particles is focussed into a specially designed optical set-up, in which the light scattered from the object plane is divided into two parts with the beam splitter cube 1, one for recording the light intensity distribution with the CCD1 camera and the other for analysing the Doppler shift $d\nu_L = \nu_D - \nu_L$ with the Michelson interferometer as described by Seiler and Oertel (1983) (see Fig. 2).

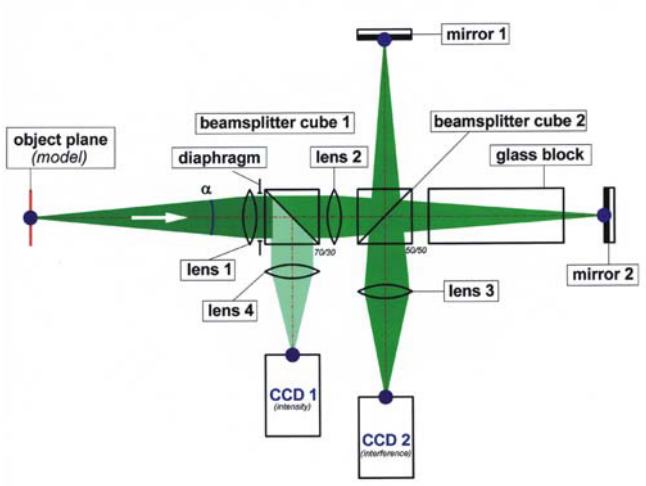

Fig. 2. Whole field Michelson interferometer.

The Michelson interferometer in Fig. 2. consists of a beam splitter cube 2 with a 50% reflecting mirror, the two mirrors M1 and M2 and the glass block G between M2 and cube 2. The scattered light coming from the object plane and passing through the lens L2 is divided by the beam splitter 2 into two parts of equal intensity. These two parts are focused by the lens L2 on M1 and M2, respectively. With the lens L3 the image of the object plane on M1 and M2 is transferred to the image plane (CCD2 camera). In this image plane the light coming from the two interferometer legs (1) and (2) interferes and the light intensity I at all image points P′, as a result of that interference, depends on the phase difference $\Delta\varphi$. This phase difference has its origin in the two legs of the Michelson interferometer as given in the following relation, with I_0 as the light intensity that is scattered by the tracer particles:

$$I = I_0 \cos^2 \frac{\Delta\varphi}{2} \text{ , normalized relation: } \frac{I}{I_0} = \cos^2 \frac{\Delta\varphi}{2} \text{ with } 0 \le \frac{I}{I_0} \le 1 \tag{2}$$

The phase difference $\Delta\varphi$ is a function of the optical path difference $\Delta\phi$, the light source frequency ν_L and the speed of light c_0 in vacuum, as follows:

$$\frac{\Delta\varphi}{2\pi} = \nu_L \frac{\Delta\phi}{c_0} \text{ with } \Delta\phi = 2n\left|l_2 - l_1\right| \tag{3}$$

The difference $l_2 - l_1$ is the geometrical path difference between the two interferometer legs. By differentiating $\Delta\varphi$ in Eq. (3) to $d\nu_L$, the expression (4) is obtained. Equation (4) explains that frequency changes $d\nu_L$, due to the Doppler effect, are directly proportional to variations $d(\Delta\varphi)$ of the phase difference $\Delta\varphi$.

$$d\left(\frac{\Delta\varphi}{2\pi}\right) = \frac{\Delta\phi}{c_0} d\nu_L \tag{4}$$

The light scattered from the light sheet plane is Doppler shifted to ν_D in the case of tracer displacement caused by flow movement. The frequency changes

$$d\nu_L = \nu_D - \nu_L \tag{5}$$

of the scattered light coming from the object plane are transformed into changes $d(\Delta\varphi)$ (see Eq. (4)) of the phase difference $\Delta\varphi$ between the two legs of the Michelson interferometer. As already stated, in Eq. (1), (3), (4) and (5), the index (L) denotes the light source, and the index (D) of the detector, i.e., the Michelson interferometer. The $d(\Delta\varphi)$ change in Eq. (4) causes variations dI of the interference light intensity I in the image plane, as:

$$dI = -\frac{I_0}{2} \sin\Delta\varphi \cdot d(\Delta\varphi) \tag{6}$$

Therefore, the light intensity distribution I in the image plane (Doppler picture), related to the initially adjusted intensity I of the reference image, informs on the frequency shift $d\nu_L$, which is proportional to the tracer speed (see Eq. (1)). This means that at all image points P' (CCD2 camera), dI is given as: dI = I (reference image) – I (Doppler picture). The Michelson interferometer is adjusted initially, before flow onset, to have interference fringes by turning the mirror M1 by a small angle β. It would be preferable to adjust the interferometer to a homogeneous light intensity output, which is a constantly distributed light intensity I in the image plane, but this is not recommended in practice because the optical components such as mirrors, lenses and cubes have only a limited optical accuracy. The best alternative is to adjust the Michelson interferometer initially to the easily obtainable interference fringe pattern mentioned above (Seiler et al., 2002).

3. High-speed Wedge Flow Visualization

3.1 Shock-tunnel Facility

The DPV technique was applied to measure the vertical velocity component over a wedge in supersonic high-speed flow. This flow was generated in the ISL/STB shock-tunnel facility by direct mode operation and a conical full-capture nozzle, which produces a short-duration (3 milliseconds) Mach-4 nitrogen flow, (see Haertig et al., 2002). 50 mm downstream of the nozzle exit, a 15° wedge is placed slightly off axis (+7 mm) into the supersonic nozzle flow producing an attached oblique shock wave over the wedge surface. That shock wave turns the incoming flow parallel to the wedge surface.

Figure 3 shows a view of the ISL shock tube laboratory with the two shock tunnels STA (left) and STB (right). A principle sketch of the ISL/STB shock-tunnel-facility, in which these experiments have been carried out, is given in Fig. 4. The shock tunnel consists of three parts: the high-pressure driver section, the driven section containing the test gas, and the nozzle attached at the end of the driven tube. As the driver gas, hydrogen at a pressure of about 13 MPa is used for the experiments reported herein. The driven tube is filled with nitrogen at a pressure of 0.22 MPa. After the burst of the diaphragm a shock wave is formed by which the test gas is accelerated in the driven section and expanded via the nozzle to flow over the wedge.

The conical nozzle used at STB opens into the test section (see Fig. 5), with the wedge mounted in front of the nozzle. This section is equipped with windows at both sides and at the top. A light sheet is produced from top by an Nd:YAG laser pulse (λ = 532 nm), see vector $\vec{e}_L$ in Fig. 6, which illuminates a plane axially oriented in the middle of the wedge flow. The observation by the Michelson interferometer was perpendicular from the side, $\vec{e}_D$, and the measured component of the flow vector $\vec{v}$ is directed vertically.

Fig. 3. Shock Tube Laboratory, aerial view (left), inside view (right).

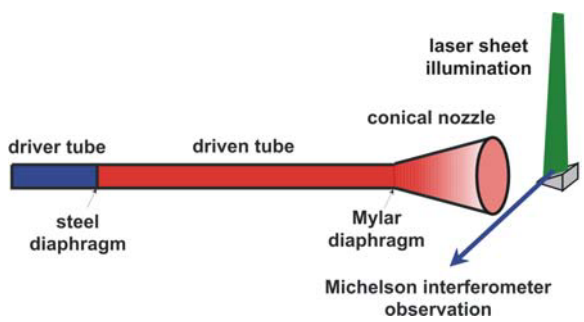

Fig. 4. Principle sketch of the shock tunnel ISL/STB.

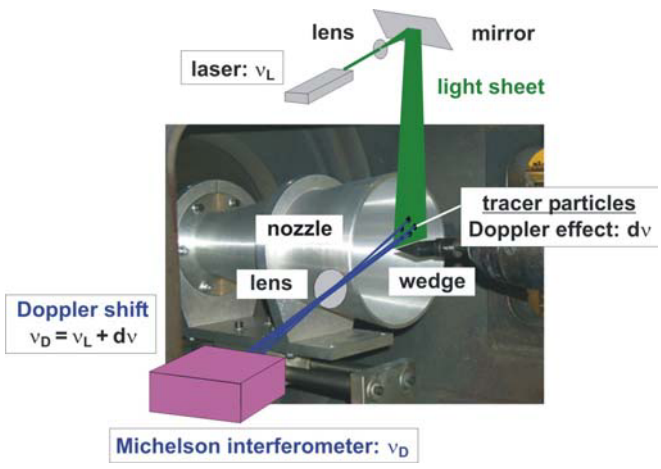

Fig. 5. Experimental arrangement.

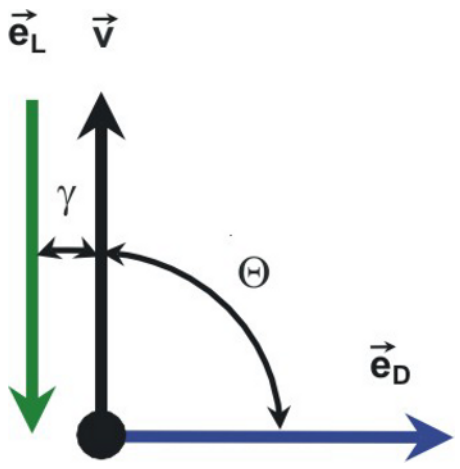

Fig. 6. Vector diagram.

3.2 Wedge Flow Visualization by DPV

In Fig. 7. the initially adjusted fringe pattern present before flow onset, the reference picture, can be seen in the light sheet plane formed over the wedge. In order to scatter the light coming from the top with frequency ν_L into the Michelson interferometer in the case of no flow (no tracers), a diffuser plate was placed over the wedge surface. The interference fringe adjustment by turning the mirror M1 is clearly visible. The fringes appear slightly curved due to optical inaccuracies.

Because of the characteristics of the conical nozzle used for the experiments, the flow around the wedge is slightly divergent resulting in a vertical flow component, superimposed to the axial nozzle flow, which is in the range of 5% of the axial velocity. Therefore, the fringe pattern in front of the oblique wedge shock wave is also Doppler-shifted. That vertical velocity causes a Doppler shift of the frequency of the light scattered by tracer particles, here titanium dioxide (TiO_2). The fringe pattern as it looks for the wedge flow is given in Fig. 8, as taken with the CCD2 camera. The wedge shock wave is clearly visible on the Doppler picture by means of a fringe shift caused by the velocity jump across the shock wave, which is attached to the tip of the wedge. Over the wedge the flow turns vertically due to the flow deflection, which results in a light intensity change across the wedge shock wave that appears as an approximately one-half fringe displacement in Fig. 8, which corresponds to about 260 nm. The processed flow region is marked in Fig. 8 and 9 by a rectangle.

Fig. 7. Doppler picture taken before flow onset.

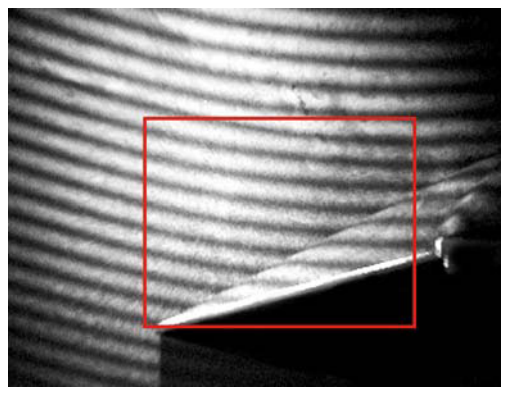

Fig. 8. Doppler picture of the wedge flow.

In gas flows, the tracer particles are commonly not distributed homogeneously, resulting in a distortion of the Doppler picture light intensity distribution I in the image plane. In order to solve this problem independently of light intensity fluctuations, which influence the amplitude I_0 in Equation (2), a picture of the light intensity distribution I_0 (see Fig. 9), is taken simultaneously with the Doppler picture. I_0 is recorded with the CCD1 camera shown in Fig. 2. In dividing the two pictures pixel-wise, the Doppler picture light intensity distribution I (see Fig. 8) is normalized by the intensity picture I_0 of Fig. 9, so that an I_0-independent Doppler picture results according to Equation (2) with $0 \le I/I_0 \le 1$. This intensity normalizing procedure is also done for the reference picture taken initially before flow onset.

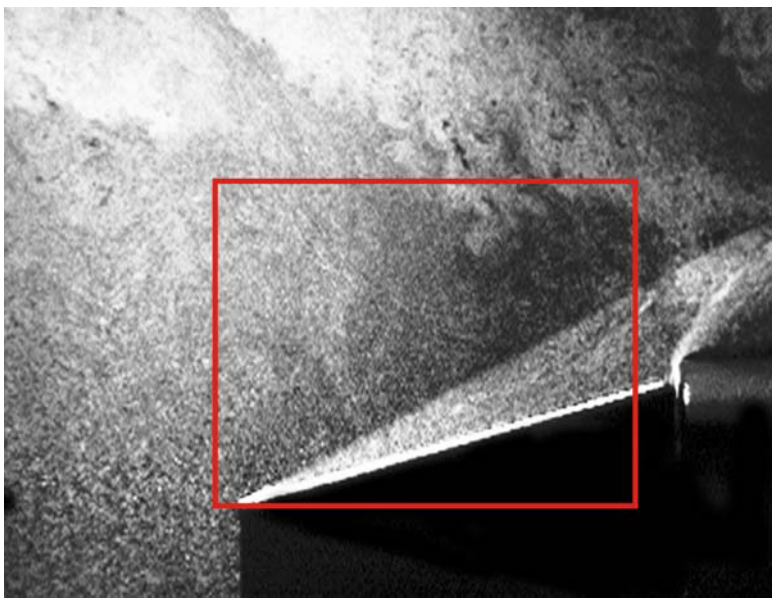

Fig. 9. Light intensity picture on the CCD1 camera.

At each pixel of the CCD2 camera (optical set-up see Fig. 2), which is used for taking the Doppler picture, the light intensity is stored and the image processing procedure explained by Leopold et al. (2000) is applied, on the one hand to normalize the Doppler picture of Fig. 8 and on the other hand to determine pixel by pixel the flow velocity distribution. Therefore, the phase difference change $d(\Delta\varphi) = \Delta\varphi_D - \Delta\varphi_L$ on the normalized Doppler picture ($\Delta\varphi_D$) is pixel-wise determined with Eq. (2) as a shift against the reference picture of Fig. 7 ($\Delta\varphi_L$). In the following, the frequency shift $d\nu_L = \nu_D - \nu_L$ is obtained by applying Eq. (4). Detailed information on the image processing procedure is given by Seiler et al. (2002). For calculating the amount of the tracer velocity $\vec{v}$ visualized with the Doppler picture in Figure 8, the relation deduced from Eq. (1) is applied at each CCD pixel as:

$$v = \frac{d\nu_L}{\nu_L}\,\frac{c}{2}\,\frac{1}{\cos\gamma\cdot\sin\theta/2} \tag{7}$$

3.3 DPV Velocity Visualization

The image processing software developed at ISL involves the picture normalization procedure mentioned before as well as some tools to overlay correctly the pictures to be processed,

see Seiler et al. (2002). Thereby the distribution of the vertical velocity component $\vec{v}$ appearing in the light sheet plane was pixel-wise determined. The result is given in Fig. 10 by means of the DPV velocity picture, which shows in pseudo colors the visualized formation of the vertical v-velocity component present in the nozzle flow in front of the oblique wedge shock wave in green and behind it over the wedge surface in red. Looking at the velocity picture in Fig. 10, deduced from the Doppler picture in Fig. 8, the velocity distribution is evaluated relative to the reference fringe system obtained before flow onset (Fig. 7). The data reduction error is estimated to about 10% of the determined velocity. The velocity results are as follows for the region in front and behind the oblique shock wave:

v-velocity: front (green): v = 100 ± 10 m/s, behind (red): v = 360 ± 36 m/s.

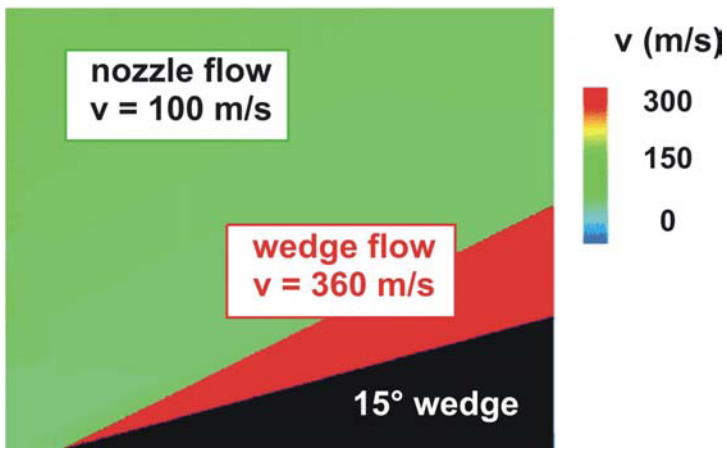

Fig. 10. DPV velocity visualization in terms of pseudo colors.

3.4 PIV Measurement of Nozzle and Wedge Flow

To obtain reliable information on the nozzle outflow velocity distribution, Particle Image Velocimetry (PIV) was applied. A detailed description of the application of the PIV method to high-speed shock-tunnel flows is given by Havermann et al. (2001). Figure 11 shows the PIV results for the horizontal velocity distribution u on the left-hand side and for the vertical velocity v on the right-hand side.

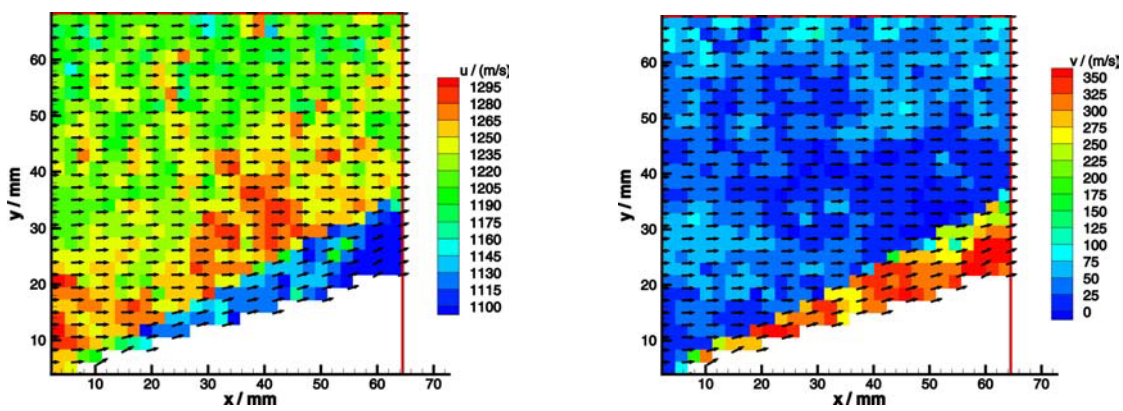

Fig. 11. Horizontal (u) and vertical (v) velocity distribution measured with PIV.

In Fig. 11, the 15° wedge ramp is located in the lower part of the diagram, seen in white and the velocity distribution measured in the light sheet plane over the wedge is shown in terms of pseudo colors. The location of the oblique shock wave in front of the wedge surface can be determined as a strong velocity jump in both pictures. The velocities in the PIV interrogation areas were averaged in front of and behind the oblique shock wave. The following data are obtained:

u-velocity: front (green/red): u = 1257 ± 36 m/s, behind (blue): u = 1135 ± 33 m/s,
v-velocity: front (blue): v = 35 ± 22 m/s, behind (yellow/red): v = 305 ± 48 m/s.

In theory, by a solution of the conservation equations it follows that the shock wave influenced wedge flow is constant. Experimentally, this prediction is confirmed by the DPV as well as the PIV measurements, (see Fig. 10 and 11.) The theoretically predicted vertical wedge flow velocity is 296 m/s, which agrees well with the PIV measurement (305 ± 48 m/s). By applying the shock tube flow calculation procedures of ISL, the flow properties at the exit of the nozzle can be determined using the experimentally obtained velocity data. From these deductions the nozzle outflow flow is characterized as:

u = 1257 m/s, v = 35 m/s, M = 4.0, p = 42 kPa, T = 240 K.

4. Comparison of DPV and PIV Results

The DPV velocity results deviate considerably from the velocity data obtained by PIV, as shown in Fig. 11. The PIV measurements yield the vertical v-velocity component v = 305 ± 48 m/s, whereas the DPV evaluation yields v = 360 ± 36 m/s. Within the given error bars both measurement results overlap, which means that the disagreement is not as remarkable as it appears. The PIV technology was successfully tested by Havermann et al. (2001) for shock tunnel flows, wherefore it can be assumed that the DPV determined v-velocity distribution is overlaid by a systematic error which originates, to our knowledge, due to the slightly unstable behavior of the reference fringe distribution in Fig. 7 during the experiment.

The DPV v-velocity seems to be overestimated by about 60 m/s, which is the difference between the DPV (front: v = 100 m/s, behind: v = 360 m/s) and PIV (front: v = 35 m/s, behind: v = 305 m/s) visualized velocity data. The DPV picture velocity overestimation of 60 m/s corresponds to a shift of about 10% of the laser wavelength (532 nm). In order to generate this wavelength shift by mechanically moving, for example, mirror M1, a displacement of the order of 50 nm is sufficient which can certainly occur during shock tube operation.

This outcome shows that for the DPV technique presently used, a systematic error of the order of about 60 m/s is overlaid to the measuring error of about 10%, resulting mainly from the data processing software. Probably due to vibrations occurring during the experimental run, the reference fringe system in Fig. 7 was found to be unstable from the moment of taking the reference picture (no flow) up to the time at which the Doppler picture (flow) is taken. Some optical parts, especially the mirrors, are possibly displaced by mechanical and/or thermal effects resulting in a shift of the optical path length difference $\Delta\phi$ (see Eq. (3)).

Therefore, with the present optical set-up only the fringe shift across the oblique shock wave, as seen in Fig. 8, can be deduced correctly as velocity jump Δv. This jump is measured by the present DPV technique to $\Delta v = 260 \pm 26$ m/s. The PIV data in Fig. 11 yield: $\Delta v = 270 \pm 35$ m/s. This outcome suggests that, at the moment, the DPV technique is only able to measure velocity changes

correctly (e.g. the jump across the oblique wedge shock), because the reference and Doppler pictures are taken at different moments and not simultaneously.

5. Conclusions

The Doppler Picture Velocimetry DPV technique was developed in 1981 with the visualization of fringe shifts showing changes in the flow velocity distribution present in a laser illuminated plane. At that time the Doppler picture evaluation only gave limited information on the velocity distribution in the flow area considered. Recently, with the enhanced DPV technique, the Doppler picture is taken with a CCD-camera and the output is treated pixel-wise using appropriate software, which is under development at ISL. Therefore, the DPV concept, using the gray values, is a tool that allows information to be obtained at any pixel of the light sheet crossing the flow investigated.

To overcome the restriction whereby only the relative velocity distribution is available at present by DPV, a new Michelson system is under development for taking the Doppler picture and the reference picture simultaneously. Consequently, the absolute velocity distribution will be obtained more precisely. A new optical set-up is in progress and will be tested in future applications of flow velocity measurements in the ISL shock-tunnel facilities (see Seiler et al., 2002).

The new DPV set-up uses three CCD cameras, CCD1 for taking the interference fringes resulting from the Doppler shifted frequency of the scattered light, CCD2 for taking the reference picture, which uses unshifted laser light and CCD3 for taking the intensity distribution of the scattered light. The light passing the Michelson interferometer is polarized in order to separate the Doppler-shifted light and the reference light, which originates from a dispersion plate that is directly illuminated by the laser light source.

References

Oertel, H., Seiler, F. and George, A., Visualisierung von Geschwindigkeitsfeldern mit Dopplerbildern, (Visualization of Velocity Fields with Doppler Pictures), ISL-Report R 115/82, (1982).

Seiler, F. and Oertel, H., Visualization of velocity fields with Doppler-pictures, proc. 3rd International Symposium on Flow Visualization, Ann Arbor, Michigan, USA (1983).

Seiler, F., Srulijes, J. and George, A., A Doppler-picture Camera for Velocity Field Visualization, Proc. 12th International Congress on Instrumentation in Aerospace Simulation Facilities, Williamsburg, VA, USA, (1987).

Merzkirch, W., Laser -Speckle-Velocimetrie, In Lasermethoden in der Strömungsmechanik, Hrsg. B, Ruck, AT-Fachverlag, Stuttgart (1990).

Seiler, F., Srulijes, J. and George, A., Principles of Laser Velocimetry with Doppler-pictures, Proc. SPIE's 36th Annual International Symposium on Optical and Optoelectronic Science and Engineering, San Diego, California, USA, (1991).

Meyers, J. F., Doppler Global Velocimetry the Next Generation, AIAA 92-3897, (1992).

Seiler, F., George, A. and Srulijes, J., Doppler Picture Interference Velocimetry (DPV), Proc. 8th International Symposium on Flow Visualization, Sorrento, Italy, (1998).

Seiler, F., George, A., Leopold, F., Srulijes, J. and Smeets, G., Velocity Field Visualization using Doppler Picture Interference Velocimetry, proc. 18th International Congress on Instrumentation in Aerospace Simulation Facilities (ICIASF), Toulouse, France, ISL-Report PU 331/99, (1999).

Leopold, F., Seiler, F., Schneider, A. and Srulijes, J., Traitement des Images Doppler Interférentielles, remove 7ème Congrès Francophone de Vélocimetrie Laser, Marseille, France, (2000)

Havermann, M., Haertig, J., Rey, C. and George, A., Particle Image Velocimetry (PIV) Applied to High Speed Shock Tunnel Flows, proc. 23rd International Symposium on Shock Waves, Fort Worth, Tx, USA, (2001).

Seiler, F., George, A., Leopold, F., Havermann, M. and Srulijes, J., Enhanced Doppler Picture Velocimetry (DPV) for Planar Velocity Measurements in High Speed Shock Tunnel Flow, Proc. The 10th International Symposium on Flow Visualization, August 26-29, Kyoto, Japan, (2002).

Haertig, J., Havermann, M., Rey, C. and George, A., Particle Image Velocimetry in Mach 3.5 and 4.5 Shock Tunnel Flows, AIAA Journal, 40-6 (2002), 1056-1060.

Author Profile

Friedrich Seiler: He received his "Dipl.-Phys." degree in 1975 and his "Dr.-Ing." degree in 1980 from the University of Karlsruhe, Germany. In 1992, he became a lecturer in fluid mechanics, and in 1998, a professor at the same university. Since 1980, he has been a scientist at the French-German Research Institute of Saint-Louis (ISL), France. From 1998, he has been head of the Shock Tube Department.

Marc Havermann: He received his degree as Diplom-Ingenieur in Mechanical Engineering in 1994 and his PhD in Mechanical Engineering in 1999 from the RWTH Aachen, Germany. In 1999 he started as a research scientist in the Shock Tube Dept. of the French-German Research Institute of Saint-Louis, France. His work deals with flows in shock tunnels and optical flow diagnostics.

Alfred George: He was born in Rielasingen, Germany, in 1947. In 1967, he received a technical degree from the Lyceum in Saint-Louis, France. The same year he joined the Franco-German Research Institute ISL in Saint Louis, France. He has been involved in several optical measurement problems applied to high-speed gas dynamics.

Friedrich Leopold: He was born in Freudenstadt, Germany, on April 27, 1963. He received his Dipl.-Ing. Degree in aeronautical engineering from the University Stuttgart, in 1989. In 1993, he received his Doctorate degree from the University Braunschweig. Since 1989, he works in the aerodynamic department of the French-German Research Institute (ISL).

Julio Srulijes: Mechanical Engineering degree, Buenos Aires (RA) in 1972. 1979 Dr.-Ing. degree, University of Karlsruhe (D). 1980-83 University of Essen (D). Since 1984 French-German Research Institute of Saint-Louis (F). He works on gas dynamics of high enthalpy flows at the Shock Tube Laboratory. He participated in the development of several optical measurement techniques.